Perturbation Learning Based Anomaly Detection

Anonymous Author(s)
Affiliation
Address
email

Abstract

This paper presents a simple yet effective method for anomaly detection. The main idea is to learn small perturbations to perturb normal data and learn a classifier to classify the normal data and the perturbed data into two different classes. The perturbator and classifier are jointly learned using deep neural networks. Importantly, the perturbations should be as small as possible but the classifier is still able to recognize the perturbed data from unperturbed data. Therefore, the perturbed data are regarded as abnormal data and the classifier provides a decision boundary between the normal data and abnormal data, although the training data do not include any abnormal data. Compared with the state-of-the-art of anomaly detection, our method does not require any assumption about the shape (e.g. hypersphere) of the decision boundary and has fewer hyper-parameters to determine. Empirical studies on benchmark datasets verify the effectiveness and superiority of our method.

1 Introduction

Anomaly detection (AD) is an important research problem in many areas such as computer vision, machine learning, and chemical engineering [Chandola *et al.*, 2009; Ramachandra *et al.*, 2020; Pang *et al.*, 2021; Ruff *et al.*, 2021]. AD aims to identify abnormal data from normal data and is usually an unsupervised learning task because the anomaly samples are unknown in the training stage. In the past decades, numerous AD methods [Schölkopf *et al.*, 1999, 2001; Breunig *et al.*, 2000; Liu *et al.*, 2008] have been proposed. For instance, one-class support vector machine (OCSVM) [Schölkopf *et al.*, 2001] maps the data into high-dimensional feature space induced by kernels and tries to find a hyperplane giving possibly maximal distance between the normal data and the origin. Tax and Duin [2004] proposed a method called support vector data description (SVDD), which finds the smallest hyper-sphere encasing the normal data in the high-dimensional feature space. SVDD is similar to OCSVM with Gaussian kernel function.

Classical anomaly detection methods such as OCSVM and SVDD are generally not suitable for large-scale data due to the high computational costs, and are not effective to deal with more complex data such as those in vision scenarios. To address these issues, a few researchers Erfani *et al.* [2016]; Golan and El-Yaniv [2018]; Abati *et al.* [2019]; Wang *et al.* [2019]; Qiu *et al.* [2021] attempted to take advantages of deep learning [LeCun *et al.*, 2015; Goodfellow *et al.*, 2016] to improve the performance of anomaly detection. One typical way is to use deep auto-encoder or its variants[Vincent *et al.*, 2008; Kingma and Welling, 2013; Pidhorskyi *et al.*, 2018; Wang *et al.*, 2021] to learn effective data representation or compression models. Auto-encoder and its variants have achieved promising performance in AD. In fact, these methods do not explicitly define an objective for anomaly detection. Instead, they usually use the data reconstruction error as a metric to detect anomalies.

There are a few approaches to building deep anomaly detection objectives or models. Typical examples include classical one-class learning based approach[Ruff *et al.*, 2018, 2019; Perera and Patel, 2019; Bhattacharya *et al.*, 2021], probability estimation based approach [Zong *et al.*, 2018; Pérez-Cabo *et al.*, 2019; Su *et al.*, 2019], and adversarial learning based approach [Deecke *et al.*, 2018;

Submitted to 36th Conference on Neural Information Processing Systems (NeurIPS 2022). Do not distribute.

Perera *et al.*, 2019; Raghuram *et al.*, 2021]. For example, Ruff *et al.* [2018] proposed deep one-class classification (DSVDD), which applies deep neural network to learn an effective embedding for the normal data such that in the embedding space, the normal data can be encased by a hyper-sphere with minimum radius. The deep autoencoding Gaussian mixture model (DAGMM) proposed by Zong *et al.* [2018] is composed of a compression network and an estimation network based on Gaussian mixture model. The anomaly scores are described as the output energy of the estimation network. Perera *et al.* [2019] proposed one-class GAN (OCGAN) to learn a latent space to represent a specific class by adversarially training the auto-encoder and discriminator. The properly trained OCGAN network can well reconstruct the specific class of data, while failing to reconstruct other classes of data. Moreover, some latest works also explore interesting perspectives. Goyal *et al.* [2020] proposed the method called deep robust one-class classification (DROCC). DROCC assumes that the normal samples generally lie on low-dimensional manifolds, and regards the process of finding the optimal hyper-sphere in the embedding space as an adversarial optimization problem. Yan *et al.* [2021] claimed that anomalous domains generally exhibit different semantic patterns compared with the peripheral domains, and proposed the semantic context based anomaly detection network (SCADN) to learn the semantic context from the masked data via adversarial learning. Chen *et al.* [2022] proposed the interpolated Gaussian descriptor (IGD) to learn more valid data descriptions from representative normal samples rather than edge samples. Shenkar and Wolf [2022] utilized contrastive learning to construct the method called generic one-class classification (GOCC) for AD on tabular data. It is worth noting that classical AD methods such as OCSVM [Schölkopf *et al.*, 2001] and DSVDD [Ruff *et al.*, 2018] require specific assumptions (e.g. hypersphere) for the distribution or structure of the normal data. The GAN-based approaches [Deecke *et al.*, 2018; Perera *et al.*, 2019] suffer from the instability problem of min-max optimization and have high computational costs.

In this paper, we propose a novel AD method called perturbation learning based anomaly detection (PLAD). PLAD aims to learn a perturbator and a classifier from the normal training data. The perturbator uses minimum effort to perturb the normal data to abnormal data while the classifier is able to classify the normal data and perturbed data into two classes correctly. The main contributions of our work are summarized as follows:

- We propose a novel AD method called PLAD. PLAD does not require any assumption about the shape of the decision boundary between the normal data and abnormal data. In addition, PLAD has much fewer hyper-parameters than many state-of-the-art AD methods such as [Wang *et al.*, 2019; Goyal *et al.*, 2020; Yan *et al.*, 2021].
- We propose to learn perturbations directly from the normal training data. For every training data point, we learn a distribution from which any sample can lead to a perturbation such that the normal data point is flipped to an abnormal data point.
- Besides the conventional empirical studies on one-class classification, we investigate the performance of our PLAD and its competitors in recognizing abnormal data from multi-class normal data. These results show that our PLAD has state-of-the-art performance.

2 Proposed method

Suppose we have a distribution $\mathcal{D}$ of d dimension and any data drawn from $\mathcal{D}$ are deemed as normal data. Now we have some training data $\mathbb{X} = \{\mathbf{x}_1, \mathbf{x}_2, \ldots, \mathbf{x}_n\}$ randomly drawn from $\mathcal{D}$ and we want to learn a discriminative function f from $\mathbb{X}$ such that $f(\mathbf{x}) > 0$ for any $\mathbf{x} \in \mathcal{D}$ and $f(\mathbf{x}) < 0$ for any $\mathbf{x} \notin \mathcal{D}$. This is an unsupervised learning problem and also known as anomaly detection, where any $\mathbf{x} \notin \mathcal{D}$ are deemed as abnormal data.

In contrast to classical anomaly detection methods such as one-class SVM [Schölkopf *et al.*, 2001], deep SVDD [Ruff *et al.*, 2018] , and DROCC [Goyal *et al.*, 2020], in this paper, we do not make any assumption about the distribution $\mathcal{D}$. Inspired from the generative adversarial learning [Goodfellow *et al.*, 2014], we propose to learn a discriminator that is able to recognize fake data (abnormal data) and a generator that is able to fool the discriminator, but the input of the generator is real data (normal data), which is essentially different from GAN. To be more precise, we propose to learn perturbations for $\mathbf{X}$ such that the perturbed $\mathbb{X}$ (denoted by $\widetilde{\mathbb{X}} = \{\tilde{\mathbf{x}}_1, \tilde{\mathbf{x}}_2, \ldots, \tilde{\mathbf{x}}_n\}$) are abnormal but quite close to $\mathbb{X}$. To ensure the abnormality of $\widetilde{\mathbb{X}}$, we learn a classifier f from $\{\mathbb{X}, \widetilde{\mathbb{X}}\}$ such that $f(\mathbf{x}) > 0$ for any $\mathbf{x} \in \mathbb{X}$ and $f(\tilde{\mathbf{x}}) < 0$ for any $\tilde{\mathbf{x}} \in \widetilde{\mathbb{X}}$. To ensure that $\widetilde{\mathbb{X}}$ is close to $\mathbb{X}$, the perturbations should be small

enough. Therefore, we propose to solve the following problem

$$\underset{\theta,\,\widetilde{\mathbb{X}}}{\text{minimize}}\ \frac{1}{n}\sum_{i=1}^{n}\ell(y_i, f_\theta(\mathbf{x}_i)) + \frac{1}{n}\sum_{i=1}^{n}\ell(\tilde{y}_i, f_\theta(\tilde{\mathbf{x}}_i)) + \frac{\lambda}{n}\sum_{i=1}^{n}\phi(\mathbf{x}_i, \tilde{\mathbf{x}}_i), \tag{1}$$

where $\ell(\cdot,\cdot)$ denotes some loss function such as cross-entropy and $y_1 = \cdots = y_n = 0$ and $\tilde{y}_1 = \cdots = \tilde{y}_n = 1$ are the labels for the normal data and perturbed data respectively. λ is a hyperparameter to control the magnitudes of the perturbations. θ denotes the set of parameters of the classifier f and $\phi(\cdot,\cdot)$ is some distance metric quantifying the difference between two data points. However, directly solving (1) encounters the following difficulties.

- First, the number $(|\theta| + dn)$ of decision variables to optimize can be huge if n is large, where $|\theta|$ denotes the cardinality of the set θ.
- Second, it is hard to use mini-batch optimization because some decision variables (i.e. $\widetilde{\mathbb{X}}$) are associated with the sample indices.
- Lastly, it is not easy to determine ϕ because ϕ relies on the unknown distribution $\mathcal{D}$. For instance, $\phi(\mathbf{x}, \tilde{\mathbf{x}}) = \|\mathbf{x} - \tilde{\mathbf{x}}\|^2$, namely the squared Euclidean norm, does not work if $\mathbb{X}$ is enclosed by a hypersphere or hypercube (data points close to the centroid require much larger perturbations than those far away from the centroid, which implies that $\mathbf{x} - \tilde{\mathbf{x}}$ has a non-Gaussian distribution).

To overcome these three difficulties, we propose to solve the following problem instead

$$\begin{aligned}&\underset{\theta,\,\tilde{\theta}}{\text{minimize}}\ \frac{1}{n}\sum_{i=1}^{n}\ell(y_i, f_\theta(\mathbf{x}_i)) + \frac{1}{n}\sum_{i=1}^{n}\ell(\tilde{y}_i, f_\theta(\tilde{\mathbf{x}}_i)) + \frac{\lambda}{n}\sum_{i=1}^{n}\left(\|\boldsymbol{\alpha}_i - \mathbf{1}\|^2 + \|\boldsymbol{\beta}_i - \mathbf{0}\|^2\right)\\ &\text{subject to}\ \ \tilde{\mathbf{x}}_i = \mathbf{x}_i \odot \boldsymbol{\alpha}_i + \boldsymbol{\beta}_i,\ (\boldsymbol{\alpha}_i, \boldsymbol{\beta}_i) = g_{\tilde{\theta}}(\mathbf{x}_i),\ i = 1, 2, \ldots, n,\end{aligned} \tag{2}$$

where $\mathbf{1} = [1, 1, \ldots, 1]^\top$ and $\mathbf{0} = [0, 0, \ldots, 0]^\top$ are d-dimensional constant vectors and $\odot$ denotes the Hadamard product of two vectors. $\boldsymbol{\alpha}_i$ and $\boldsymbol{\beta}_i$ are multiplicative and additive perturbations for $\mathbf{x}_i$ and they are generated from a perturbator $g_{\tilde{\theta}}$, where $\tilde{\theta}$ denotes the set of parameters to learn. In (2), we hope that the multiplicative perturbation is close to 1 and the additive perturbation is close to zero but they relies on the data point $\mathbf{x}$. Therefore, the perturbation learning is adaptive to the unknown distribution $\mathcal{D}$, which solves the third aforementioned difficulty.

In fact, problem (2) can be reformulated as

$$\begin{aligned}\underset{\theta,\,\tilde{\theta}}{\text{minimize}}\ \ &\frac{1}{n}\sum_{i=1}^{n}\Big(\ell\big(y_i, f_\theta(\mathbf{x}_i)\big) + \ell\big(\tilde{y}_i, f_\theta(\mathbf{x}_i \odot g^{\alpha}_{\tilde{\theta}}(\mathbf{x}_i) + g^{\beta}_{\tilde{\theta}}(\mathbf{x}_i))\big)\Big)\\ &+ \frac{\lambda}{n}\sum_{i=1}^{n}\Big(\|g^{\alpha}_{\tilde{\theta}}(\mathbf{x}_i) - \mathbf{1}\|^2 + \|g^{\beta}_{\tilde{\theta}}(\mathbf{x}_i) - \mathbf{0}\|^2\Big),\end{aligned} \tag{3}$$

where $\begin{bmatrix} g^{\alpha}_{\tilde{\theta}}(\mathbf{x}_i) \\ g^{\beta}_{\tilde{\theta}}(\mathbf{x}_i)\end{bmatrix} = g_{\tilde{\theta}}(\mathbf{x}_i)$, $i = 1, 2, \ldots, n$. We see that we only need to optimize the parameters θ and $\tilde{\theta}$ and the total number of decision variables is $|\theta| + |\tilde{\theta}|$, which solved the first difficulty we discussed previously. On the other hand, θ and $\tilde{\theta}$ are not associated with the sample indices, which solved the second difficulty. Once f_θ and $g_{\tilde{\theta}}$ are learned, we can then use f_θ to detect whether a new data point $\mathbf{x}_{\text{new}}$ is normal (e.g. $f_\theta(\mathbf{x}_{\text{new}}) < 0.5$) or abnormal (e.g. $f_\theta(\mathbf{x}_{\text{new}}) > 0.5$). We call the method *Perturbation Learning based Anomaly Detection* (PLAD).

In PLAD, namely (3), both the classifier f_θ and the perturbator $g_{\tilde{\theta}}$ are neural networks. They can be fully connected neural networks, convolutional neural networks (for image data anomaly detection), or recurrent neural networks (for sequential data anomaly detection). Figure 1 shows the motivation of our PLAD and the network architecture. Compared with many popular anomaly detection methods, our PLAD has the following characteristics.

- PLAD does not make any assumption about the distribution or structure of the normal data. In contrast, one-class SVM [Schölkopf *et al.*, 2001], deep SVDD [Ruff *et al.*, 2018], and DROC-C [Goyal *et al.*, 2020] make specific assumptions about the distribution of the normal data, which may be violated in real applications. For example, deep SVDD assumes that the normal data are encased by a hypersphere, which is hard to guarantee in real applications and may require a very deep neural network to transform a non-hypersphere structure to a hypersphere structure.

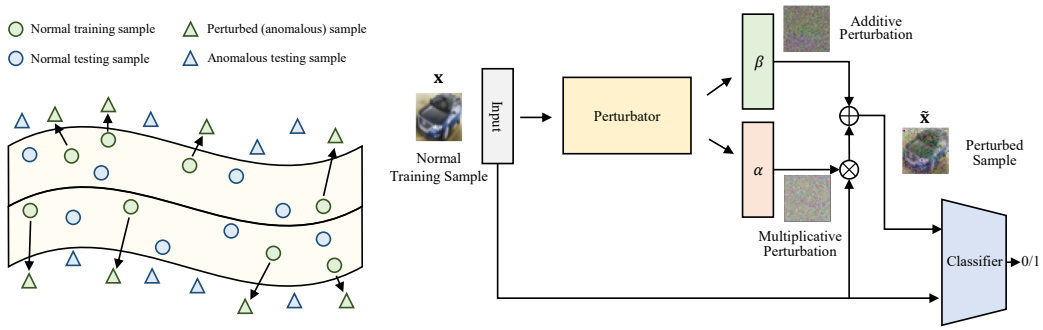

Figure 1: The motivation and network architecture of the proposed PLAD method.

- In PLAD, besides the network structures, we only need to determine one hyperparameter λ, which provides huge convenience in real applications. In contrast, many state-of-the-art AD methods such as [Wang *et al.*, 2019; Goyal *et al.*, 2020; Yan *et al.*, 2021] have at least two key hyperparameters. For example, in DROCC [Goyal *et al.*, 2020], one has to determine the radius of hyper-sphere, the step size of gradient-ascent, and two regularization parameters.
- In PLAD, we can use gradient based optimizer such as Adam to solve the optimization. The time complexity is comparable to that of vanilla deep neural networks (for classification or representation). On the contrary, many recent advances DROCC [Goyal *et al.*, 2020] of anomaly detection especially those GAN based methods [Deecke *et al.*, 2018; Perera *et al.*, 2019; Yan *et al.*, 2021] have much higher computational cost.

In the left of Figure 1, actually, a normal training data can be perturbed to an abnormal data by different perturbations. Therefore, we propose to learn a distribution from which any perturbations can perturb the normal training data to be abnormal. Specifically, for every $\mathbf{x}_i$, there exists a distribution Ω_i, such that for any $\mathbf{z} \in \Omega_i$, the perturbation given by $(\boldsymbol{\alpha}, \boldsymbol{\beta}) = h(\boldsymbol{z})$ can perturb $\mathbf{x}_i$ to be abnormal, where h is a nonlinear function modelled by a neural network. We can just assume that Ω_i is a Gaussian distribution with mean $\boldsymbol{\mu}_i$ and variance $\boldsymbol{\sigma}_i^2$, i.e., $\Omega_i = \mathcal{N}(\boldsymbol{\mu}_i, \boldsymbol{\sigma}_i^2)$, because of the universal approximation ability of h. We take the idea of variational autoencoder (VAE) [Kingma and Welling, 2013] and minimize

$$\mathcal{L}(\tilde{\theta}_1, \tilde{\theta}_2) = D_{KL}\left(q_{\tilde{\theta}_1}(\mathbf{z}|\mathbf{x}) \| p(\mathbf{z})\right) - \mathbb{E}_{q_{\tilde{\theta}_2}(\mathbf{z}|\mathbf{x})}\left[\log p_{\tilde{\theta}_2}(\boldsymbol{\varepsilon}|\mathbf{z})\right], \tag{4}$$

where $p(\mathbf{z}) = \mathcal{N}(\mathbf{0}, \mathbf{1})$, $\boldsymbol{\varepsilon} = \begin{bmatrix}\mathbf{1}\\ \mathbf{0}\end{bmatrix}$, $\mathbf{z} = l_{\tilde{\theta}_1}(\mathbf{x})$, $(\boldsymbol{\alpha}, \boldsymbol{\beta}) = h_{\tilde{\theta}_2}(\mathbf{z})$, $\tilde{\theta}_1$ are the parameters of the encoder l, and $\tilde{\theta}_2$ are the parameters of the decoder h. Combing (4) with (3), we have $\tilde{\theta} = \{\tilde{\theta}_1, \tilde{\theta}_2\}$ and solve

$$\begin{aligned} \underset{\theta,\, \tilde{\theta}}{\text{minimize}} \quad & \frac{1}{n}\sum_{i=1}^{n}\Big(\ell\big(y_i, f_\theta(\mathbf{x}_i)\big) + \ell\big(\tilde{y}_i, f_\theta(\mathbf{x}_i \odot g_{\tilde{\theta}}^{\alpha}(\mathbf{x}_i) + g_{\tilde{\theta}}^{\beta}(\mathbf{x}_i))\big)\Big) \\ & + \frac{1}{n} D_{KL}\left(q_{\tilde{\theta}_1}(\mathbf{z}|\mathbf{x}) \| p(\mathbf{z})\right) - \lambda \mathbb{E}_{q_{\tilde{\theta}_2}(\mathbf{z}|\mathbf{x})}\left[\log p_{\tilde{\theta}_2}(\boldsymbol{\varepsilon}|\mathbf{z})\right], \end{aligned} \tag{5}$$

where $g_{\tilde{\theta}} = h_{\tilde{\theta}_2} \circ l_{\tilde{\theta}_1}$. The training is similar to that for VAE [Kingma and Welling, 2013] and will not be detailed here.

It should be pointed out that the method (5) is just an extension of the method (3). In (5), we want to learn a distribution for each normal training data point $\mathbf{x}_i$ such that any perturbations generated from the distribution can perturb $\mathbf{x}_i$ to be abnormal. It is expected that (5) can outperform (3) in real applications. The corresponding experiments are in the supplementary material.

3 Connection with previous works

The well-known one-class classification methods such as OCSVM [Schölkopf *et al.*, 2001], DSVD-D [Ruff *et al.*, 2018] and DROCC [Goyal *et al.*, 2020] have specific assumptions for the embedded

distribution while our PLAD does not require any assumption and is able to adaptively learn a decision boundary even if it is very complex. It is also noteworthy that the idea of DROCC in identifying anomalies is similar to ours, i.e, training a classifier instead of an auto-encoder or embedding model.

Self-supervised learning based methods, e.g., GOAD [Bergman and Hoshen, 2020] NeuTraL AD [Qiu *et al.*, 2021], etc., work through designing an appropriate auxiliary task to help the model to learn useful data features. Both our approach and the self-supervised learning based methods aim to learn a binary classifier on the original data and auxiliary data. But they are different in the following two points. First, in self-supervised learning (e.g. contrastive learning) based methods, the auxiliary data are generated by some pre-defined and manual operations (e.g. image rotation and cropping). In contrast, in our approach, the auxiliary data are adaptively and dynamically learned from the original data. Second, self-supervised learning based methods are often designed for some specific types of data such as image data, whereas it may be difficult to generate auxiliary data for other types of data. In contrast, it is easy to apply our approach to any type of data.

Adversarial learning based methods [Malhotra *et al.*, 2016; Deecke *et al.*, 2018; Pidhorskyi *et al.*, 2018; Perera *et al.*, 2019] are generally constructed with auto-encoder and generative adversarial networks (GANs) [Goodfellow *et al.*, 2014], and the most widely used measure of them to detect anomalies is the reconstruction error. Compared with them, we exploit the idea of VAE when producing perturbations and the detection metric is a classifier, which should be more suitable than reconstruction error for anomaly detection. On the other hand, in these adversarial learning based AD methods, the min-max optimization leads to instabilities in detecting anomalies, while the optimization of PLAD is much easier to solve. Another interesting work SCADN [Yan *et al.*, 2021] tries to produce negative samples by multi-scale striped masks to train a GAN, but its anomaly score still relies on reconstruction error and the production of masks has randomness or may be hard to determine in various real scenarios. Our PLAD learns perturbations adaptively from the data itself, which is convenient and reliable.

4 Experiment

In this section, we evaluate the proposed method in comparison to several state-of-the-art anomaly detection methods on two image datasets and two tabular datasets. Note that all the compared methods do not utilize any pre-trained feature extractors.

4.1 Datasets and baseline methods

Datasets description

- **CIFAR-10:** CIFAR-10 image dataset is composed of 60,000 images in total, where 50,000 samples for training and 10,000 samples for test. It includes 10 different balanced classes.
- **Fashion-MNIST:** Fashion MNIST contains 10 different categories of grey-scale fashion style objects. The data is split into 60,000 images for training and 10,000 images for test.
- **Thyroid:** Thyroid is a hypothyroid disease dataset that contains 3,772 samples with 3 classes and 6 attributes. We follow the data split settings of [Zong *et al.*, 2018] to preprocess the data for one-class classification task.
- **Arrhythmia:** Arrhythmia dataset consists of 452 samples with 274 attributes. Here we also follow the data split settings of [Zong *et al.*, 2018] to preprocess the data.

The detailed information of each dataset is illustrated in Table 1.

Table 1: Details of the datasets used in our experiments.

Dataset name	Type	# Total samples	# Dimension
CIFAR-10	Image	60,000	$32\times32\times3$
Fashion-MNIST	Image	70,000	28×28
Thyroid	Tabular	3,772	6
Arrhythmia	Tabular	452	274

Baselines and state-of-the-arts. We compare our method with the following classical baseline methods and state-of-the-art methods: OCSVM [Schölkopf *et al.*, 2001], isolation forest (IF) [Liu *et al.*, 2008], local outlier factor (LOF) [Breunig *et al.*, 2000], denoising auto-encoder (DAE)[Vincent *et al.*, 2008], E2E-AE and DAGMM [Zong *et al.*, 2018], DCN [Caron *et al.*, 2018], ADGAN [Deecke *et al.*, 2018], DSVDD [Ruff *et al.*, 2018], OCGAN [Perera *et al.*, 2019], TQM [Wang *et al.*, 2019], GOAD [Bergman and Hoshen, 2020], DROCC [Goyal *et al.*, 2020], HRN-L2 and HRN [Hu *et al.*, 2020], SCADN [Yan *et al.*, 2021], IGD (Scratch) [Chen *et al.*, 2022], NeuTraL AD [Qiu *et al.*, 2021], and GOCC [Shenkar and Wolf, 2022].

4.2 Implementation details and evaluation metrics

In this section, we first describe the implementation details of the proposed PLAD method. The settings for image and tabular datasets are illustrated as follows:

- **Image datasets.** For image datasets (CIFAR-10 and Fashion-MNIST), we utilize the LeNet-based CNN to construct the classifier, which is same as [Ruff *et al.*, 2018] and [Goyal *et al.*, 2020] to provide fair comparison. And we apply the MLP-based VAE to learn the noise for data. Since both image datasets contains 10 different classes, it can be regard as 10 independent one-class classification tasks, and each task on CIFAR-10 have 5,000 training samples (6,000 for Fashion-MNIST) and 10,000 testing samples for both of them. Consequently, the choice of optimizer (from Adam [Kingma and Ba, 2015] and SGD), learning rate and hyper-parameter λ could be varies for different classes. The suggested settings of them on each experiment in this paper refer to the supplementary material.
- **Tabular datasets.** For tabular datasets (Thyroid and Arrhythmia), we both use the MLP-based classifier and VAE in practice, and we uniformly train them with Adam optimizer and learning rate of 0.001. Besides, λ is set to 3 for Thyroid and 2 for Arrhythmia.

For the competitive methods in the experiment, we report their performance directly from the following paper [Hu *et al.*, 2020; Goyal *et al.*, 2020; Yan *et al.*, 2021; Qiu *et al.*, 2021; Chen *et al.*, 2022; Shenkar and Wolf, 2022] except for DROCC, which we run the official released code to obtain the results. Due to the limitation of paper length, the details of the our network settings are provided in the supplementary material.

For the selection of evaluation metrics, we follow the previous works such as [Ruff *et al.*, 2018] and [Zong *et al.*, 2018] to use AUC (Area Under the ROC curve) for image datasets and F1-score for tabular datasets because the anomaly detection for image and tabular datasets has different evaluation criteria. Moreover, our method does not need pre-training like [Ruff *et al.*, 2018] and others did, so we uniformly train the proposed method 5 times with 100 epochs to obtain the average performance and standard deviation. Note that we run all experiments on NVIDIA RTX3080 GPU with 32GB RAM, CUDA 11.0 and cuDNN 8.0.

4.3 Experimental results

4.3.1 Experiment on image datasets

Table 2 and Table 3 summarize the average AUCs performance of the one-class classification tasks on CIFAR-10 and Fashion-MNIST, where we have the following observations:

- Compared with some classical shallow model-based approaches such OCSVM and IF, the proposed PLAD method significantly outperforms them on each one-class classification task with a large margin. This is mainly due to the powerful feature learning capability of deep neural network.
- PLAD also explicitly outperforms several well-known deep anomaly detection methods such as DAGMM and DSVDD, and consistently obtains the top two AUC scores on most classes of CIFAR-10 and Fashion-MNIST compared to some latest methods such as TQM, DROCC and HRN. Specifically, in the class "Automobile" of CIFAR-10 and class "Sandal" of Fashion-MNIST, the proposed method exceeds 5.9% and 4.7% in terms of AUC compared to the runner-up. We also conduct statistical analysis for our method against other competitors, the detailed analysis refers to the supplementary material due to the page limitations.
- It is noteworthy that some deep anomaly detection methods such as DSVDD and DROCC, are mainly based on the assumption that the normal data in the embedding space are situated in a hyper-

Table 2: Average AUCs (%) in one-class anomaly detection on CIFAR-10. Note that for the competitive methods we only report their mean performance, while we further report the standard deviation for the proposed method. * denotes we run the official released code to obtain the results, and the best two results are marked in **bold**.

Normal Class	Airplane	Auto mobile	Bird	Cat	Deer	Dog	Frog	Horse	Ship	Truck
OCSVM [Schölkopf *et al.*, 2001]	61.6	63.8	50.0	55.9	66.0	62.4	74.7	62.6	74.9	75.9
IF [Liu *et al.*, 2008]	66.1	43.7	64.3	50.5	74.3	52.3	70.7	53.0	69.1	53.2
DAE[Vincent *et al.*, 2008]	41.1	47.8	61.6	56.2	72.8	51.3	68.8	49.7	48.7	37.8
DAGMM [Zong *et al.*, 2018]	41.4	57.1	53.8	51.2	52.2	49.3	64.9	55.3	51.9	54.2
ADGAN [Deecke *et al.*, 2018]	63.2	52.9	58.0	60.6	60.7	65.9	61.1	63.0	74.4	64.2
DSVDD [Ruff *et al.*, 2018]	61.7	65.9	50.8	59.1	60.9	65.7	67.7	67.3	75.9	73.1
OCGAN [Perera *et al.*, 2019]	75.7	53.1	64.0	62.0	72.3	62.0	72.3	57.5	82.0	55.4
TQM [Wang *et al.*, 2019]	40.7	53.1	41.7	58.2	39.2	62.6	55.1	63.1	48.6	58.7
DROCC* [Goyal *et al.*, 2020]	79.2	**74.9**	**68.3**	62.3	70.3	66.1	68.1	**71.3**	62.3	**76.6**
HRN-L2 [Hu *et al.*, 2020]	**80.6**	48.2	64.9	57.4	**73.3**	61.0	74.1	55.5	79.9	71.6
HRN [Hu *et al.*, 2020]	77.3	69.9	60.6	**64.4**	71.5	**67.4**	**77.4**	64.9	**82.5**	77.3
PLAD	**82.5** (0.4)	**80.8** (0.9)	**68.8** (1.2)	**65.2** (1.2)	**71.6** (1.1)	**71.2** (1.6)	**76.4** (1.9)	**73.5** (1.0)	**80.6** (1.8)	**80.5** (1.3)

Table 3: Average AUCs (%) and in one-class anomaly detection on Fashion-MNIST. Note that for some competitive methods we only report their mean performance, while we further report the standard deviation for the proposed method and several reproduced methods. * denotes we run the official released code to obtain the results, and the best two results are marked in **bold**. The p-value of t-test is also included to perform statistical analysis for our method against others.

Normal Class	T-shirt	Trouser	Pullover	Dress	Coat	Sandal	Shirt	Sneaker	Bag	Ankle boot
OCSVM [Schölkopf *et al.*, 2001]	86.1	93.9	85.6	85.9	84.6	81.3	78.6	97.6	79.5	97.8
IF [Liu *et al.*, 2008]	91.0	97.8	87.2	93.2	90.5	93.0	80.2	98.2	88.7	95.4
DAE[Vincent *et al.*, 2008]	86.7	97.8	80.8	91.4	86.5	92.1	73.8	97.7	78.2	96.3
DAGMM [Zong *et al.*, 2018]	42.1	55.1	50.4	57.0	26.9	70.5	48.3	83.5	49.9	34.0
ADGAN [Deecke *et al.*, 2018]	89.9	81.9	87.6	91.2	86.5	89.6	74.3	97.2	89.0	97.1
DSVDD [Ruff *et al.*, 2018]	79.1	94.0	83.0	82.9	87.0	80.3	74.9	94.2	79.1	93.2
DSVDD* [Ruff *et al.*, 2018]	78.4±3.3	93.6±1.3	80.8±3.4	84.1±2.0	85.9±2.4	82.0±3.0	75.0±3.8	94.5±1.8	80.6±5.9	94.1±1.5
OCGAN [Perera *et al.*, 2019]	85.5	93.4	85.0	88.1	85.8	88.5	77.5	93.9	82.7	97.8
TQM [Wang *et al.*, 2019]	92.2	95.8	**89.9**	93.0	**92.2**	89.4	**84.4**	98.0	**94.5**	98.3
DROCC* [Goyal *et al.*, 2020]	88.1±3.3	97.7±0.7	87.6±1.4	87.7±1.6	87.2±2.2	91.0±1.6	77.1±2.0	95.3±0.7	82.7±2.9	95.9±2.1
HRN-L2 [Hu *et al.*, 2020]	91.5	97.6	88.2	92.7	91.0	71.9	79.4	**98.9**	90.8	**98.9**
HRN [Hu *et al.*, 2020]	**92.7**	98.5	88.5	93.1	92.1	**91.3**	79.8	**99.0**	**94.6**	98.8
HRN* [Hu *et al.*, 2020]	88.8±0.1	**98.6±0.1**	84.8±0.1	**93.2±0.1**	89.5±0.2	89.6±0.1	74.4±0.1	98.9±0.0	87.2±0.3	97.7±0.1
PLAD	**93.1±0.5**	**98.6±0.2**	**90.2±0.7**	**93.7±0.6**	**92.8±0.8**	**96.0±0.4**	**82.0±0.6**	98.6±0.3	90.9±1.0	**99.1±0.1**
p-value (t-test)	T-shirt	Trouser	Pullover	Dress	Coat	Sandal	Shirt	Sneaker	Bag	Ankle boot
v.s. DSVDD	1.5×10^{-7}	1.2×10^{-6}	2.2×10^{-5}	1.0×10^{-7}	2.1×10^{-5}	8.2×10^{-8}	8.7×10^{-4}	4.7×10^{-5}	0.003	2.9×10^{-6}
v.s. DROCC	9.4×10^{-4}	0.004	3.3×10^{-4}	3.4×10^{-6}	3.0×10^{-5}	3.1×10^{-6}	4.4×10^{-4}	3.4×10^{-7}	9.9×10^{-6}	5.1×10^{-4}
v.s. HRN	4.0×10^{-9}	0.614	1.2×10^{-7}	0.013	5.9×10^{-6}	3.0×10^{-10}	1.5×10^{-9}	5.4×10^{-4}	2.2×10^{-5}	1.7×10^{-10}

sphere, while anomalies are outside the sphere. Therefore the edge of the hyper-sphere is then the decision boundary learned by the model to identify anomalies. In contrast, PLAD does not require any assumption about the shape of the decision boundary. It attempts to learn the perturbation from data itself by neural network and construct the anomalies by enforcing the perturbation to original data, then train network to distinguish the normal samples and anomalies. Of course, this is also natural to associate PLAD with some adversarial learning based methods such as ADGAN and OCGAN, etc. In contrast to them, the optimization of PLAD is a non-adversary problem, because it tries to simultaneously minimize the perturbation to produce the anomalies that similar to normal ones and minimize the cross-entropy to distinguish them.

Moreover, Table 4 also shows the average performance on CIFAR-10 and Fashion-MNIST over all 10 classes to provide an overall comparison. Note that we further compare with two latest methods SCADN and IGD (Scratch). They do not included in the above two tables because the performance on each class is not provided in the paper. From this table we can observe that PLAD achieves the best average AUCs on both datasets among all competitive methods.

We also apply t-SNE [Van der Maaten and Hinton, 2008] to visualize the learned embedded space in Figure 2. Specifically, we visualize the training samples of a specific category, perturbed data for training samples, as well as all test samples. They are divided into three sub-figures for ease

Table 4: Average AUCs (%) over all 10 classes on CIFAR-10 and Fashion-MNIST. Note that the best two results are marked in **bold**.

Data set	CIFAR-10	Fashion-MNIST
OCSVM [Schölkopf *et al.*, 2001]	64.7	87.0
IF [Liu *et al.*, 2008]	59.7	91.5
DAE[Vincent *et al.*, 2008]	53.5	88.1
DAGMM [Zong *et al.*, 2018]	53.1	51.7
ADGAN [Deecke *et al.*, 2018]	62.4	88.4
DSVDD [Ruff *et al.*, 2018]	64.8	84.7
OCGAN [Perera *et al.*, 2019]	65.6	87.8
TQM [Wang *et al.*, 2019]	52.1	92.7
DROCC* [Goyal *et al.*, 2020]	69.9	89.0
HRN-L2 [Hu *et al.*, 2020]	66.6	90.0
HRN [Hu *et al.*, 2020]	71.3	**92.8**
SCADN [Yan *et al.*, 2021]	66.9	—
IGD (Scratch) [Chen *et al.*, 2022]	**74.3**	92.0
PLAD	**75.1**	**93.5**

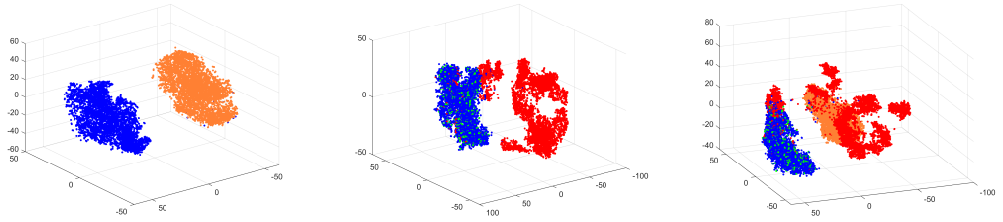

(a) Training v.s. perturbed (b) Training v.s. test (c) Training v.s. perturbed v.s. test

Figure 2: The learned embedded space visualized by t-SNE. Note the points marked in blue, orange, green, and red are training samples, perturbed samples, normal test samples, and anomalous test samples, respectively. We select the class of "Sneaker" in Fashion-MNIST to provide the visualization. More results for the other categories can be found in the supplementary material.

of understanding. Figure 2 shows the visualization of the the class "Sneaker" in Fashion-MNIST. More results can be found on the supplementary material. From this figure we have the following observations. First, PLAD obviously learns good decision boundary for distinguishing normal data and perturbed data from Figure 2(a). Second, Figures 2(b) and 2(c) show that the normal test samples lie in the same manifold as the training samples, while the abnormal samples (abnormal test samples and perturbed samples) are relatively separated. In other words, PLAD explicitly learns a discriminative embedded space to distinguish normal samples and anomalies.

4.3.2 Experiment on non-image datasets

Table 5 summarizes the F1-scores of each competitive method on the Thyroid and Arrhythmia datasets. It can be observed that PLAD significantly outperforms several baseline methods such as OCSVM, DAGMM, DSVDD and DROCC with a large margin. Although NeuTraL AD and GOCC achieve encouraging 76.8% F1-score on Thyroid, it is worth mentioning that they are both methods designed for non-image data. The Arrhythmia dataset seems to be a more difficult anomaly detection task because of its small sample size, which is not conducive to deep learning. Surprisingly, the proposed PLAD method show remarkable performance on Arrhythmia, which surpasses 9.2% compared to the runner-up. Moreover, the performance of PLAD is also comparable to NeuTraL AD and GOCC on Thyroid, which fully demonstrates its applicability to the anomaly detection task for non-image data.

4.3.3 Experiment on separate anomaly from multi-class normal data

It should be pointed out that in real applications, the normal data may contains multiple classes without labels. We need to separate anomaly from these multi-class normal data. In this study,

Table 5: Average F1-scores (%) with the standard deviation per method on two tabular datasets (Thyroid and Arrhythmia). * denotes we run the official released code to obtain the results, and the best two results are marked in **bold**.

Data set	Thyroid	Arrhythmia
OCSVM [Schölkopf *et al.*, 2001]	39.0 ± 1.0	46.0 ± 0.0
LOF [Breunig *et al.*, 2000]	54.0 ± 1.0	51.0 ± 1.0
E2E-AE[Zong *et al.*, 2018]	13.0 ± 4.0	45.0 ± 3.0
DCN [Caron *et al.*, 2018]	33.0 ± 3.0	38.0 ± 3.0
DAGMM [Zong *et al.*, 2018]	49.0 ± 4.0	49.0 ± 3.0
DSVDD [Ruff *et al.*, 2018]	73.0 ± 0.0	54.0 ± 1.0
DROCC* [Goyal *et al.*, 2020]	68.7 ± 2.3	32.3 ± 1.8
GOAD [Bergman and Hoshen, 2020]	74.5 ± 1.1	52.0 ± 2.3
NeuTraL AD [Qiu *et al.*, 2021]	$\mathbf{76.8} \pm \mathbf{1.9}$	60.3 ± 1.1
GOCC [Shenkar and Wolf, 2022]	$\mathbf{76.8} \pm \mathbf{1.2}$	$\mathbf{61.8} \pm \mathbf{1.8}$
PLAD	76.6 ± 0.6	$\mathbf{71.0} \pm \mathbf{1.7}$

we randomly select 10,000 samples among the training split of CIFAR-10 or Fashion-MNIST to construct a new normal training set, namely, the normal data are in multiple classes. Subsequently, we randomly select two samples from the test split of CIFAR-10 or Fashion-MNIST to construct 10,000 anomalous samples using the means of pair-wise samples in pixel level. The produced anomalous samples are merged with the original test split to form a new test set. Compared with the previous two tasks (Sections 4.3.1 and 4.3.2), this one is much more difficult because the decision boundary between the anomalous samples and the normal samples are very complicated. We run the experiment to compare our method with four baselines including OCSVM, DAGMM, DSVDD and DROCC and report the results in Table 6. We see that the proposed PLAD method outperforms the baselines significantly. Foe example, the improvement over the runner-up DSVDD is 9.1% and 4.4% on CIFAR-10 and Fashion-MNIST. The success of PLAD mainly stem from the ability of learning a decision boundary adaptively without any assumption.

Table 6: AUCs (%) of the experiment of separating anomaly from multi-class normal data.

Data set	CIFAR-10	Fashion-MNIST
OCSVM [Schölkopf *et al.*, 2001]	54.9 ± 0.0	64.8 ± 0.0
DAGMM [Zong *et al.*, 2018]	44.3 ± 0.6	49.2 ± 2.6
DSVDD [Ruff *et al.*, 2018]	63.6 ± 1.1	70.9 ± 2.0
DROCC [Goyal *et al.*, 2020]	60.9 ± 5.8	68.1 ± 3.1
PLAD	$\mathbf{72.7} \pm \mathbf{1.9}$	$\mathbf{75.3} \pm \mathbf{2.8}$

5 Conclusion

We have presented a novel method PLAD for anomaly detection. Compared with its competitors, PLAD does not require any assumption about the distribution or structure of the normal data. This is the major reason for that PLAD outperforms its competitors. In addition, PLAD has fewer hyperparameters to determine and has lower computation cost than many strong baselines such as [Wang *et al.*, 2019; Goyal *et al.*, 2020; Yan *et al.*, 2021]. Actually, PLAD provides us a framework for anomaly detection. Different neural networks such as CNN [Krizhevsky *et al.*, 2012], RNN [Mikolov *et al.*, 2010], GNN [Scarselli *et al.*, 2008], and even transformer Vaswani *et al.* [2017] can be embedded into PLAD to accomplish various anomaly detection tasks such as time series anomaly detection. One limitation of our work is that we haven't included these experiments currently. Note that in this study, we only considered the additive and multiplicative perturbations, i.e., $\tilde{\mathbf{x}} = \mathbf{x} \odot g_{\tilde{\theta}}^{\alpha}(\mathbf{x}) + g_{\tilde{\theta}}^{\beta}(\mathbf{x})$, while a more general perturbation can be formulated as $\tilde{\mathbf{x}} = g_{\tilde{\theta}}'(\mathbf{x})$. When we need a very sophisticated perturbator, we may not well approximate $g_{\tilde{\theta}}'(\mathbf{x})$ by $\mathbf{x} \odot g_{\tilde{\theta}}^{\alpha}(\mathbf{x}) + g_{\tilde{\theta}}^{\beta}(\mathbf{x})$, because we have to made some restriction for $g_{\tilde{\theta}}^{\alpha}$ and $g_{\tilde{\theta}}^{\beta}$. Therefore, future study may also focus on determining the ϕ for (1), to learn $g_{\tilde{\theta}}'(\mathbf{x})$ more effectively.

References

Davide Abati, Angelo Porrello, Simone Calderara, and Rita Cucchiara. Latent space autoregression for novelty detection. In *Proceedings of the IEEE/CVF Conference on Computer Vision and Pattern Recognition*, pages 481–490, 2019.

Liron Bergman and Yedid Hoshen. Classification-based anomaly detection for general data. In *Proceedings of the International Conference on Learning Representations*, 2020.

Arindam Bhattacharya, Sumanth Varambally, Amitabha Bagchi, and Srikanta Bedathur. Fast one-class classification using class boundary-preserving random projections. In *Proceedings of the 27th ACM SIGKDD Conference on Knowledge Discovery & Data Mining*, pages 66–74, 2021.

Markus M Breunig, Hans-Peter Kriegel, Raymond T Ng, and Jörg Sander. Lof: identifying density-based local outliers. In *Proceedings of the 2000 ACM SIGMOD International Conference on Management of Data*, pages 93–104, 2000.

Mathilde Caron, Piotr Bojanowski, Armand Joulin, and Matthijs Douze. Deep clustering for unsupervised learning of visual features. In *Proceedings of the European Conference on Computer Vision*, pages 132–149, 2018.

Varun Chandola, Arindam Banerjee, and Vipin Kumar. Anomaly detection: A survey. *ACM Computing Surveys (CSUR)*, 41(3):1–58, 2009.

Yuanhong Chen, Yu Tian, Guansong Pang, and Gustavo Carneiro. Deep one-class classification via interpolated gaussian descriptor. In *Proceedings of the AAAI Conference on Artificial Intelligence*, 2022.

Lucas Deecke, Robert Vandermeulen, Lukas Ruff, Stephan Mandt, and Marius Kloft. Image anomaly detection with generative adversarial networks. In *Joint European Conference on Machine Learning and Knowledge Discovery in Databases*, pages 3–17. Springer, 2018.

Sarah M Erfani, Sutharshan Rajasegarar, Shanika Karunasekera, and Christopher Leckie. High-dimensional and large-scale anomaly detection using a linear one-class svm with deep learning. *Pattern Recognition*, 58:121–134, 2016.

Izhak Golan and Ran El-Yaniv. Deep anomaly detection using geometric transformations. *Advances in Neural Information Processing Systems*, 31, 2018.

Ian Goodfellow, Jean Pouget-Abadie, Mehdi Mirza, Bing Xu, David Warde-Farley, Sherjil Ozair, Aaron Courville, and Yoshua Bengio. Generative adversarial nets. *Advances in Neural Information Processing Systems*, 27, 2014.

Ian Goodfellow, Yoshua Bengio, and Aaron Courville. *Deep learning*. MIT press, 2016.

Sachin Goyal, Aditi Raghunathan, Moksh Jain, Harsha Vardhan Simhadri, and Prateek Jain. Drocc: Deep robust one-class classification. In *Proceedings of the International Conference on Machine Learning*, pages 3711–3721. PMLR, 2020.

Wenpeng Hu, Mengyu Wang, Qi Qin, Jinwen Ma, and Bing Liu. Hrn: A holistic approach to one class learning. *Advances in Neural Information Processing Systems*, 33:19111–19124, 2020.

Diederik P Kingma and Jimmy Ba. Adam: A method for stochastic optimization. In *Proceedings of the International Conference on Learning Representations*, 2015.

Diederik P Kingma and Max Welling. Auto-encoding variational bayes. *arXiv preprint arXiv:1312.6114*, 2013.

Alex Krizhevsky, Ilya Sutskever, and Geoffrey E Hinton. Imagenet classification with deep convolutional neural networks. *Advances in Neural Information Processing Systems*, 25, 2012.

Yann LeCun, Yoshua Bengio, and Geoffrey Hinton. Deep learning. *Nature*, 521(7553):436–444, 2015.

Fei Tony Liu, Kai Ming Ting, and Zhi-Hua Zhou. Isolation forest. In *Proceedings of the IEEE International Conference on Data Mining*, pages 413–422. IEEE, 2008.

Pankaj Malhotra, Anusha Ramakrishnan, Gaurangi Anand, Lovekesh Vig, Puneet Agarwal, and Gautam Shroff. Lstm-based encoder-decoder for multi-sensor anomaly detection. *arXiv preprint arXiv:1607.00148*, 2016.

Tomas Mikolov, Martin Karafiát, Lukas Burget, Jan Cernockỳ, and Sanjeev Khudanpur. Recurrent neural network based language model. In *Interspeech*, volume 2, pages 1045–1048. Makuhari, 2010.

Guansong Pang, Chunhua Shen, Longbing Cao, and Anton Van Den Hengel. Deep learning for anomaly detection: A review. *ACM Computing Surveys (CSUR)*, 54(2):1–38, 2021.

Pramuditha Perera and Vishal M Patel. Learning deep features for one-class classification. *IEEE Transactions on Image Processing*, 28(11):5450–5463, 2019.

Pramuditha Perera, Ramesh Nallapati, and Bing Xiang. Ocgan: One-class novelty detection using gans with constrained latent representations. In *Proceedings of the IEEE/CVF Conference on Computer Vision and Pattern Recognition*, pages 2898–2906, 2019.

Daniel Pérez-Cabo, David Jiménez-Cabello, Artur Costa-Pazo, and Roberto J López-Sastre. Deep anomaly detection for generalized face anti-spoofing. In *Proceedings of the IEEE/CVF Conference on Computer Vision and Pattern Recognition Workshops*, pages 0–0, 2019.

Stanislav Pidhorskyi, Ranya Almohsen, and Gianfranco Doretto. Generative probabilistic novelty detection with adversarial autoencoders. *Advances in Neural Information Processing Systems*, 31, 2018.

Chen Qiu, Timo Pfrommer, Marius Kloft, Stephan Mandt, and Maja Rudolph. Neural transformation learning for deep anomaly detection beyond images. In *Proceedings of the International Conference on Machine Learning*, pages 8703–8714. PMLR, 2021.

Jayaram Raghuram, Varun Chandrasekaran, Somesh Jha, and Suman Banerjee. A general framework for detecting anomalous inputs to dnn classifiers. In *Proceedings of the International Conference on Machine Learning*, pages 8764–8775. PMLR, 2021.

Bharathkumar Ramachandra, Michael Jones, and Ranga Raju Vatsavai. A survey of single-scene video anomaly detection. *IEEE Transactions on Pattern Analysis and Machine Intelligence*, 2020.

Lukas Ruff, Robert Vandermeulen, Nico Goernitz, Lucas Deecke, Shoaib Ahmed Siddiqui, Alexander Binder, Emmanuel Müller, and Marius Kloft. Deep one-class classification. In *Proceedings of the International Conference on Machine Learning*, pages 4393–4402. PMLR, 2018.

Lukas Ruff, Robert A Vandermeulen, Nico Görnitz, Alexander Binder, Emmanuel Müller, Klaus-Robert Müller, and Marius Kloft. Deep semi-supervised anomaly detection. In *Proceedings of the International Conference on Learning Representations*, 2019.

Lukas Ruff, Jacob R Kauffmann, Robert A Vandermeulen, Grégoire Montavon, Wojciech Samek, Marius Kloft, Thomas G Dietterich, and Klaus-Robert Müller. A unifying review of deep and shallow anomaly detection. *Proceedings of the IEEE*, 2021.

Franco Scarselli, Marco Gori, Ah Chung Tsoi, Markus Hagenbuchner, and Gabriele Monfardini. The graph neural network model. *IEEE Transactions on Neural Networks*, 20(1):61–80, 2008.

Bernhard Schölkopf, Robert C Williamson, Alex Smola, John Shawe-Taylor, and John Platt. Support vector method for novelty detection. *Advances in Neural Information Processing Systems*, 12, 1999.

Bernhard Schölkopf, John C Platt, John Shawe-Taylor, Alex J Smola, and Robert C Williamson. Estimating the support of a high-dimensional distribution. *Neural Ccomputation*, 13(7):1443–1471, 2001.

Tom Shenkar and Lior Wolf. Anomaly detection for tabular data with internal contrastive learning. In *Proceedings of the International Conference on Learning Representations*, 2022.

Ya Su, Youjian Zhao, Chenhao Niu, Rong Liu, Wei Sun, and Dan Pei. Robust anomaly detection for multivariate time series through stochastic recurrent neural network. In *Proceedings of the 25th ACM SIGKDD International Conference on Knowledge Discovery & Data Mining*, pages 2828–2837, 2019.

David MJ Tax and Robert PW Duin. Support vector data description. *Machine Learning*, 54(1):45–66, 2004.

Laurens Van der Maaten and Geoffrey Hinton. Visualizing data using t-sne. *Journal of Machine Learning Research*, 9(11), 2008.

Ashish Vaswani, Noam Shazeer, Niki Parmar, Jakob Uszkoreit, Llion Jones, Aidan N Gomez, Łukasz Kaiser, and Illia Polosukhin. Attention is all you need. *Advances in Neural Information Processing Systems*, 30, 2017.

Pascal Vincent, Hugo Larochelle, Yoshua Bengio, and Pierre-Antoine Manzagol. Extracting and composing robust features with denoising autoencoders. In *Proceedings of the 25th International Conference on Machine Learning*, pages 1096–1103, 2008.

Jingjing Wang, Sun Sun, and Yaoliang Yu. Multivariate triangular quantile maps for novelty detection. *Advances in Neural Information Processing Systems*, 32:5060–5071, 2019.

Shaoyu Wang, Xinyu Wang, Liangpei Zhang, and Yanfei Zhong. Auto-ad: Autonomous hyperspectral anomaly detection network based on fully convolutional autoencoder. *IEEE Transactions on Geoscience and Remote Sensing*, 60:1–14, 2021.

Xudong Yan, Huaidong Zhang, Xuemiao Xu, Xiaowei Hu, and Pheng-Ann Heng. Learning semantic context from normal samples for unsupervised anomaly detection. In *Proceedings of the AAAI Conference on Artificial Intelligence*, volume 35, pages 3110–3118, 2021.

Bo Zong, Qi Song, Martin Renqiang Min, Wei Cheng, Cristian Lumezanu, Daeki Cho, and Haifeng Chen. Deep autoencoding gaussian mixture model for unsupervised anomaly detection. In *Proceedings of the International Conference on Learning Representations*, 2018.

Checklist

The checklist follows the references. Please read the checklist guidelines carefully for information on how to answer these questions. For each question, change the default **[TODO]** to [Yes] , [No] , or [N/A] . You are strongly encouraged to include a **justification to your answer**, either by referencing the appropriate section of your paper or providing a brief inline description. For example:

- Did you include the license to the code and datasets? [Yes] See Section.
- Did you include the license to the code and datasets? [No] The code and the data are proprietary.
- Did you include the license to the code and datasets? [N/A]

Please do not modify the questions and only use the provided macros for your answers. Note that the Checklist section does not count towards the page limit. In your paper, please delete this instructions block and only keep the Checklist section heading above along with the questions/answers below.

1. For all authors...
   (a) Do the main claims made in the abstract and introduction accurately reflect the paper's contributions and scope? [Yes]
   (b) Did you describe the limitations of your work? [Yes] See Section 5.
   (c) Did you discuss any potential negative societal impacts of your work? [N/A]
   (d) Have you read the ethics review guidelines and ensured that your paper conforms to them? [Yes]
2. If you are including theoretical results...

(a) Did you state the full set of assumptions of all theoretical results? [N/A]
(b) Did you include complete proofs of all theoretical results? [N/A]

3. If you ran experiments...
   (a) Did you include the code, data, and instructions needed to reproduce the main experimental results (either in the supplemental material or as a URL)? [Yes]
   (b) Did you specify all the training details (e.g., data splits, hyperparameters, how they were chosen)? [Yes]
   (c) Did you report error bars (e.g., with respect to the random seed after running experiments multiple times)? [Yes]
   (d) Did you include the total amount of compute and the type of resources used (e.g., type of GPUs, internal cluster, or cloud provider)? [Yes]
4. If you are using existing assets (e.g., code, data, models) or curating/releasing new assets...
   (a) If your work uses existing assets, did you cite the creators? [Yes]
   (b) Did you mention the license of the assets? [N/A]
   (c) Did you include any new assets either in the supplemental material or as a URL? [N/A]
   (d) Did you discuss whether and how consent was obtained from people whose data you're using/curating? [N/A]
   (e) Did you discuss whether the data you are using/curating contains personally identifiable information or offensive content? [N/A]
5. If you used crowdsourcing or conducted research with human subjects...
   (a) Did you include the full text of instructions given to participants and screenshots, if applicable? [N/A]
   (b) Did you describe any potential participant risks, with links to Institutional Review Board (IRB) approvals, if applicable? [N/A]
   (c) Did you include the estimated hourly wage paid to participants and the total amount spent on participant compensation? [N/A]